High-quality recording of bioelectric events

Part 2 Low-noise, low-power multichannel amplifier design

A. C. Metting van Rijn A. Peper C. A. Grimbergen

Laboratory of Medical Physics, University of Amsterdam, Academic Medical Centre, Meibergdreef 15, 1105 AZ Amsterdam, The Netherlands

Abstract—*A multichannel instrumentation amplifier, developed to be used in a miniature universal eight-channel amplifier module, is described. After discussing the specific properties of a bioelectric recording, the difficulties of meeting the demanded specifications with a design based on operational amplifiers are reviewed. Because it proved impossible to achieve the demanded combination of low noise and low power consumption using commercially available operational amplifiers, an amplifier equipped with an input stage with discrete transistors was developed. A new design concept was used to expand the design to a multichannel version with an equivalent input noise voltage of 0·35 μV RMS in a bandwidth of 0·1–100 Hz and a power consumption of 0·6 mW per channel. The results of this study are applied to miniature, universal, eight-channel amplifier modules, manufactured with thick-film production techniques. The modules can be coupled to satisfy the demand for a multiple of eight channels. The low power consumption enables the modules to be used in all kinds of portable and telemetry measurement systems and simplifies the power supply in stationary measurement systems.*

Keywords—*Bioelectric recordings, Low noise, Low power consumption, Multichannel front end, Small dimensions*

Med. & Biol. Eng. & Comput., 1991, **29**, 433–440

1 Introduction

IN PRESENT biomedical research, recording systems with a large number of measuring channels are often required. Examples of multichannel recordings are brain mapping: EEG measurements with 20 channels (DUFFY, 1982), 28 channels (GRUZELIER *et al.*, 1988) or 36 channels (DUFF, 1980); and body surface mapping: ECG measurements with 64 channels (REEK *et al.*, 1984; SPEKHORST and SIPPENSGROENEWEGEN, 1990). Over recent years, much progress has been made in the development of the digital part of recording systems with respect to the processing of the large amount of data gathered. The quality of the analogue front end, however, has remained much the same and in many cases does not stand up to its task.

The proper measurement and amplification of bioelectric signals present some specific problems. General amplifier design techniques are well developed and extensively described in the literature. However, in designing a biomedical amplifier much attention should be paid to the special character of a bioelectric measurement.

The fact that electrodes are used as signal transducers in bioelectric recordings has important consequences for the required performance of the amplifier. Because of its impedance, offset voltage and noise contribution, the electrode/skin interface may cause various problems, especially in multichannel recordings.

First received 23rd April and in final form 23rd July 1990

2 Amplifier design criteria

The electrode/skin interface has a complex impedance between 1 kΩ and 1 MΩ at 50 Hz (ALMASI and SCHMITT, 1970; GRIMNES, 1983; GEDDES, 1972; ROSELL *et al.*, 1988). The electrode/skin impedance depends on many factors, such as skin condition and preparation. Large variations in electrode/skin impedance can be found. High electrode/skin impedances and/or large differences between the electrode/skin impedances may cause the measurement system to be susceptible to several forms of interference. The theory was extensively treated in a previous study (METTING VAN RIJN *et al.*, 1990). To ensure correct operation with typical electrode/skin impedances and typical interference sources, an amplifier should meet the following demands:

(*a*) very high common-mode input impedance (> 100 MΩ at 50 Hz*)

(*b*) high differential-mode input impedance (> 10 MΩ at 50 Hz†)

** The common-mode input impedance of an amplifier at 50 Hz is generally determined by the input capacitance. Consequently an input capacitance of less than 33 pF is required. It will be clear that a proper guarding circuit (which virtually eliminates the cable capacitance) is inevitable if shielded cables are used (typical capacitance of shielded cable is 100 pF m^{-1})*

† The differential-mode input impedance of an amplifier is irrelevant for the susceptibility of the circuit to line interference. However, a low differential input impedance loads the electrode/skin signal sources, which may lead to input voltage reduction and distortion

(*c*) equal common-mode input impedances for all inputs
(*d*) high common mode rejection ratio (>80 dB at 50 Hz)
(*e*) shielded input cables; the shields must be driven by a proper guarding circuit (MORRISON, 1977; METTING VAN RIJN *et al.*, 1990)
(*f*) additional reduction of common-mode voltage with a driven right leg circuit (WINTER and WEBSTER, 1983; METTING VAN RIJN *et al.*, 1990)

The electrode/skin interface forms a galvanic half-cell (GEDDES, 1972). The exact half-cell voltage of an electrode/skin interface depends mainly on the condition of the skin and electrodes. To the signal measured between the electrodes, the difference between the half-cell voltages of the electrode/skin interfaces must be added. This voltage usually varies slowly during a recording, resulting in a low-frequency noise signal. An amplifier should suppress these relatively large (several tens of millivolts), low-frequency input signals to prevent saturation. A cutoff frequency of approximately 0·15 Hz for the high-pass filtering is commonly used for this objective.

The minimum signal magnitude that can be measured is defined in principle by the thermal noise of the electrode/skin impedance ($E_t = 1{\cdot}3 \times 10^{-3}\sqrt{R_e}\,\mu$V RMS in a bandwidth of 0·1–100 Hz). In practice, however, noise levels this low are almost never obtained due to variations in the half-cell voltage of the electrode/skin interface. To be able to decide about clinical death, an equivalent input noise level lower than 2 μV peak-to-peak in a bandwidth of 0·1–30 Hz is mandatory for clinical EEG amplifiers (COOPER *et al.*, 1969; SILVERMAN *et al.*, 1969). Consequently, the target value for the equivalent input noise voltage in this study is chosen to be 0·5 μV RMS in a bandwidth 0·1–100 Hz‡. An equivalent input noise current less than 5 pA RMS in a bandwidth of 0·1–100 Hz is demanded to ensure that only a small amount of noise is added with typical electrode/skin impedances (total equivalent input noise voltage is 0·6 μV RMS in a bandwidth of 0·1–100 Hz with electrode/skin impedances of 50 kΩ).

In many multichannel recordings the signal differences between each of the measuring electrodes and a common reference voltage is measured (monopolar recording). This reference voltage is sometimes derived from one electrode but often the average voltage from two (EEG) or three electrodes (ECG) is used (CLARK, 1978; GEDDES and BAKER, 1989).

Small dimensions are important for several reasons. It is obvious that small dimensions will enable the amplifier module to be used in all kinds of portable and telemetry measurements, but a small size of the amplifier also reduces the capacitance between the amplifier and its environment in an isolated amplifier setup. Reduction of this capacitance lowers the common-mode voltage, which is one of the main causes of interference (METTING VAN RIJN *et al.*, 1990).

Minimum power consumption is important because it allows small sized batteries to be used as power supply. In a system which is powered by the mains supply by the use of an isolation transformer, most of the capacitance across the isolation barrier is usually caused by the power supply (METTING VAN RIJN *et al.*, 1990). A small battery-powered amplifier can be designed to have very small capacitance to the environment, resulting in a low common-mode voltage. Another advantage is the greatly improved safety, because there are no high voltages present in the amplifier cabinet. Finally, batteries deliver a very 'clean' supply voltage, which is essential for low-noise operation (MOTCHENBACHER and FITCHEN, 1972).

‡ *The peak-to-peak value of Gaussian noise is five to six times the root-mean-square value. The noise voltage of white noise is proportional to the square root of the bandwidth of the measuring system*

3 Biomedical amplifiers with operational amplifiers

Before concentrating on multichannel amplifiers it is instructive to review the almost universally used instrumentation amplifier with three operational amplifiers, pictured in Fig. 1*a* (TOBEY *et al.*, 1971). The advantages of the circuit are:

(*a*) amplification of differential-mode signals in the first stage (gain of 20 dB or more), which makes the noise contributions from succeeding amplifier stages insignificant (MOTCHENBACHER and FITCHEN, 1972)
(*b*) no amplification of common-mode signals in the first amplifier stage. This feature makes it possible to handle common-mode voltages nearly as high as the supply voltage and to achieve a high common-mode rejection ratio without the need for precise resistor trimming (WONG and OTT, 1976)
(*c*) a high and equal common-mode input impedance for both inputs. This is an important property as differences in electrode/skin impedance and/or common-mode input impedances convert common-mode

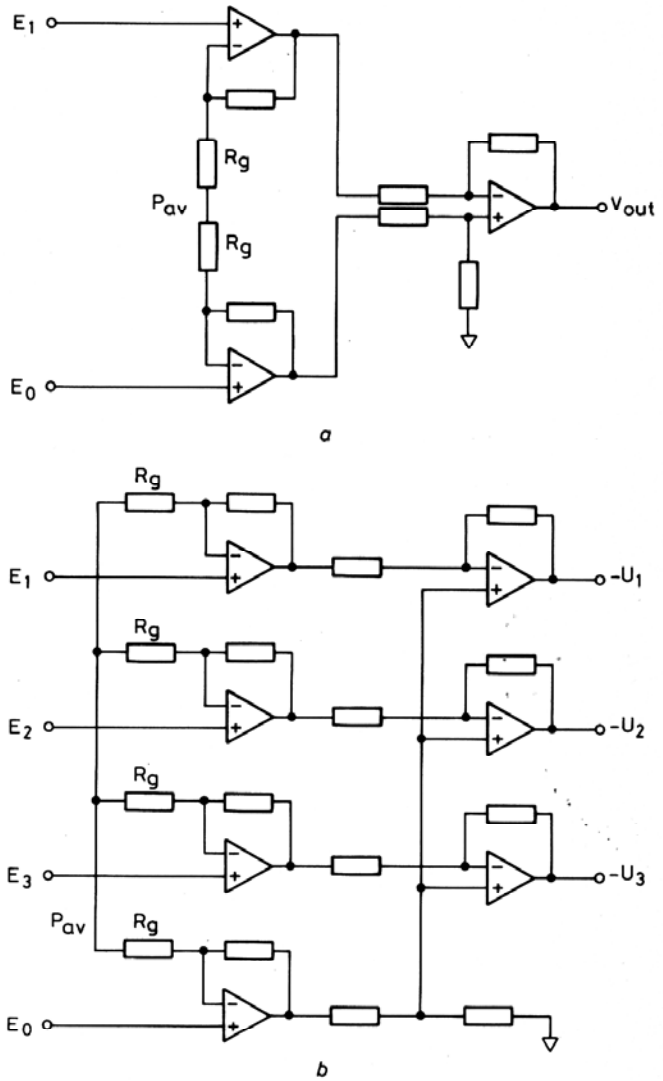

Fig. 1 *(a) Instrumentation amplifier with three operational amplifiers. Biomedical amplifiers are usually based upon this design. The voltage at point P_{av} is equal to the common-mode voltage. (b) Multichannel instrumentation amplifier with operational amplifiers. The circuit is an extension of the three operational amplifier circuit of Fig. 1a and its favourable properties are preserved*

voltage into a differential-mode voltage; this phenomenon is known as the 'potential divider effect' (PACELA, 1967; HUHTA and WEBSTER, 1973).

The three operational amplifier circuit, being widely available as a single monolithic or hybrid IC, is an attractive choice as a building block for a multichannel amplifier (SMIT *et al.*, 1987) when it is used as an independent instrumentation amplifier with its own pair of measuring electrodes (bipolar recording). However, when the potential difference between a number of electrodes and a common reference electrode is to be measured (monopolar recording, for example clinical ECG and EEG measurements) the three operational amplifier circuit is not optimal. It is tempting to interconnect several amplifier inputs to obtain a common reference input. However, this method introduces differences in common-mode input impedance between the reference input and the other (not interconnected) inputs, resulting in an increase of interference due to the 'potential divider effect' (METTING VAN RIJN *et al.*, 1990). The inclusion of a buffer amplifier at the reference input may prevent the degradation of common-mode input impedance but will add extra noise to the input signals, which are not amplified at this point.

A multichannel amplifier setup without these drawbacks is shown in Fig. 1*b*. It is basically an extension of the three operational amplifier configuration and all the favourable characteristics mentioned above are preserved (O'BRIEN *et al.*, 1983). Each input signal is amplified with respect to the voltage at point P_{av}, which voltage is equal to the average of the input voltages (= common-mode voltage). Note that all amplifier inputs are equal.

Table 1 Amplifier module specifications

Parameter	Target value	Design Fig. 3§
Equivalent input noise voltage, μV RMS, 0·1–100 Hz	<0·5	0·35
Equivalent input noise current, pA RMS, 0·1–100 Hz	<5	4
Bandwidth (+0, −3 dB), Hz	0·16–100	0·16–100
Differential mode DC input range, mV	>150	190
Differential mode AC input range, mV peak-to-peak	>20	25
Common mode input range, V peak-to-peak	>2	2·5
Input bias current, nA per input	<50	23 ± 5
Gain	500	500
Differential mode input impedance, MΩ at 50 Hz	>10	>15
Common mode input impedance:		
with unshielded input leads, MΩ at 50 Hz	>100	250
with guarded input leads MΩ at 50 Hz (cable capacitance is 330 pF)	>100	200
Common mode rejection ratio, dB at 50 Hz	>80	91 ± 5
Power consumption, mW per channel	<1	0·6

§ The results given above are measured with a supply voltage of ±7·5 V. However, the design will operate correctly with supply voltages between ±5 V and ±15 V. Higher supply voltages offer an increased AC, DC and common mode input range, at the expense of a higher power consumption, larger input bias current and a slight increase in equivalent input noise voltage and noise current

4 Biomedical amplifiers with discrete input stages

In the present study, the goal was to develop a miniature multichannel analogue front end with optimal noise properties and minimum power consumption. The specifications were based on the considerations given in Section 2 and are listed in the first column of Table 1. The design had to be suitable to be manufactured with thick-film production techniques which offer higher reliability and far smaller dimensions than printed circuit board production techniques (SERGENT, 1981).

The amplifier design shown in Fig. 1*b* seemed attractive because of its simplicity. However, with this circuit it proved impossible to achieve the desired combination of low noise and low power consumption. It can be calculated (see Appendixes 1 and 2) that it is possible in theory to surpass our specifications (Table 1) with a power consumption 10–100 times lower than offered by currently available low-noise operational amplifiers. The relatively high power consumption of operational amplifiers is mainly due to an extended bandwidth which, however, is superfluous for most physiological applications. When programmable operational amplifiers are used, they can be adjusted for a small bandwidth and low power consumption but none of these devices has an acceptable noise level**.

Therefore a multichannel instrumentation amplifier with a discrete input stage was developed. An input stage based on discrete components can offer some important advantages: the best discrete transistors are superior to the input transistors in IC operational amplifiers (NELSON, 1980) and the increased design freedom allows the input stage to be optimised for biomedical applications. In the next section a one-channel version of the amplifier is described. In addition, a new concept for expanding a one-channel instrumentation amplifier to more channels was developed. The resulting multichannel design that was used in the thick-film modules is described in Section 6.

5 One-channel instrumentation amplifier for bioelectric recordings

There was already experience gathered with a previously developed one-channel instrumentation amplifier (HAMSTRA *et al.*, 1984). Starting from that design an amplifier which met more severe specifications was developed. The circuit is shown in Fig. 2.

The input stage is based on the well known current balance amplifier circuit (WONG and OTT, 1976; GRAEME, 1977) with current sources T_3 and T_4 replacing the common-emitter resistor of the input transistors. The high output conductance of these current sources provides a very high common-mode input impedance††. The bias of T_3 is fixed; T_4 is part of the feedback circuit. In the second stage operational amplifiers are used to keep the number of parts low. The programmable operational amplifiers

** *Some modern micropower operational amplifiers (approximately 0·3 mW power consumption) specify low equivalent input noise voltage densities at 1 kHz, e.g. TLC251 (Texas Instruments): 70 nV Hz$^{-1/2}$; OP90 (PMI): 60 nV Hz$^{-1/2}$; and CA3078 (RCA): 40 nV Hz$^{-1/2}$. However, the relatively high 1/f corner frequencies (10–30 Hz) of these operational amplifiers preclude their application in low-noise biomedical amplifiers*

†† *The common mode input impedance of the design at very low frequencies is approx. $h_{FE}.R_{con}$, which works out to approx. 4 GΩ (h_{FE} is the current gain of the input transistors T_1 and T_2 (approx. 400), and R_{con} is the output conductance of the current sources T_3 and T_4 (approx. 10 MΩ)). However, at 50 Hz, the common mode input impedance is considerably lower, mainly due to the input capacitance of the input transistors T_1 and T_2 and additional stray capacitances*

used (LM4250, National Semiconductor) can be set for very low power consumption while their rather high noise is not troublesome because of the amplification in the first amplifier stage. Operational amplifier amp. A produces a single-ended output. Operational amplifiers amp. B and amp. C regulate the feedback signal. The design employs the 'current feedback' technique, which offers high common-mode rejection ratio, without the need for very precise resistor matching. Operational amplifier amp. C is used as an integrator to provide maximum feedback for direct input voltages. DC suppression without the need for large capacitors is accomplished with this circuit.

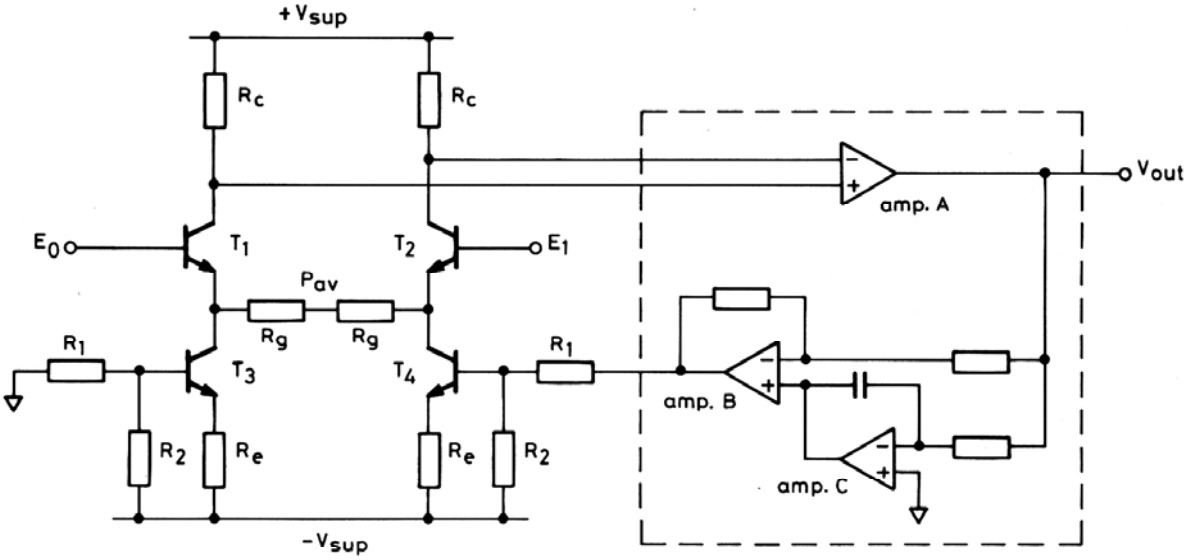

Fig. 2 *Simplified schematic of an instrumentation amplifier for biomedical applications. The combination of low noise and very low power consumption is achieved by the use of discrete transistors in the input stage*

The measured performance characteristics of the design of Fig. 2 are listed in Table 1, second column. When high-quality resistors (with a low excess noise level, see Appendix 2) are used, the equivalent input noise voltage is determined by shot-noise currents of the four transistors in the input stage only. With the use of high-quality transistors (LM194, National Semiconductor) a compromise between low noise, low power consumption, DC input range and differential-mode input impedance was obtained superior to an input stage made with operational amplifiers. A detailed description of how to find the best balance between the various specifications is given in Appendix 1.

6 Multichannel instrumentation amplifier for bioelectric recordings

When the circuit described in Section 5 is to be used in a multichannel amplifier for monopolar recordings it is again not advisable to interconnect the inputs of a number of independent instrumentation amplifiers. We developed an unconventional method to expand the design to more channels, shown for $n = 2$ in Fig. 3 (n = number of channels).

The operation of the circuit is easily understood when the behaviour of the circuit is examined with the same (common mode) signal applied to all inputs. In this case the (alternating) currents in all sections are equal and there is no voltage across the resistors R_g which interconnect the sections. Because there are no potential differences between the inputs of the operational amplifiers amp. A, all the operational amplifiers will have a zero output signal.

When differential-mode input signals (signals at the measuring inputs with respect to the reference input) are added to the common-mode signal, the voltage at point P_{av} will be equal to the average input signal (= common-mode input signal). The coupling point P_{av} in Fig. 3 is similar in this aspect to the resistor coupling point P_{av} in the design with operational amplifiers, see Fig. 1*b*. However, the differential-mode input signals produce differences in the currents between the sections. These differences in current produce potential differences between the inputs of the operational amplifiers amp. A and consequently each operational amplifier will have an output voltage proportional to the voltage between the reference electrode (input E_0) and the corresponding measuring electrode (input E_1 or E_2).

The design is a multichannel instrumentation amplifier for monopolar measurements: the amplifier has one inverting (reference) input and a number of noninverting inputs. All the important characteristics of the multichannel instrumentation amplifier with operational amplifiers (Fig. 1*b*)—no amplification of common-mode signals in the input stage, amplification of differential-mode signals in the input stage and equal common-mode input impedances for all inputs—are also present in the design depicted in Fig. 3.

The measured characteristics of the multichannel design are the same as the characteristics of the one-channel amplifier with discrete input stage (Table 1). When compared with n independent one-channel amplifiers (Fig. 2), the multichannel design of Fig. 3 offers a considerable reduction in the number of parts while the power consumption is reduced by approximately 40 per cent.

Facilities are incorporated for operation with fewer than n channels. The circuit described above does not function properly in the case of one or more badly functioning electrodes because the corresponding input sections influence the voltage at point P_{av}. Therefore, an extra input section was added (common-mode-sense section, see Fig. 3) which provides the possibility of using the amplifier in two ways. (Notation: n is the number of channels in a module, x is the number of channels that are used in the recording):

(*a*) switch in mode 'n channels', normal operation mode. $x + 1$ electrodes measuring x channels with $x = n$ (n measuring electrodes and one reference electrode). The coupling point P_{av} is driven by the $n + 1$ input transistors and the voltage at this point is the average of the input voltages (= common mode voltage). The common-mode-sense input and corresponding amplifier section are not used

(*b*) switch in mode 'x channels', optional operation mode. $x + 2$ electrodes measuring x channels with $x < n$ (x measuring electrodes, a reference electrode and a

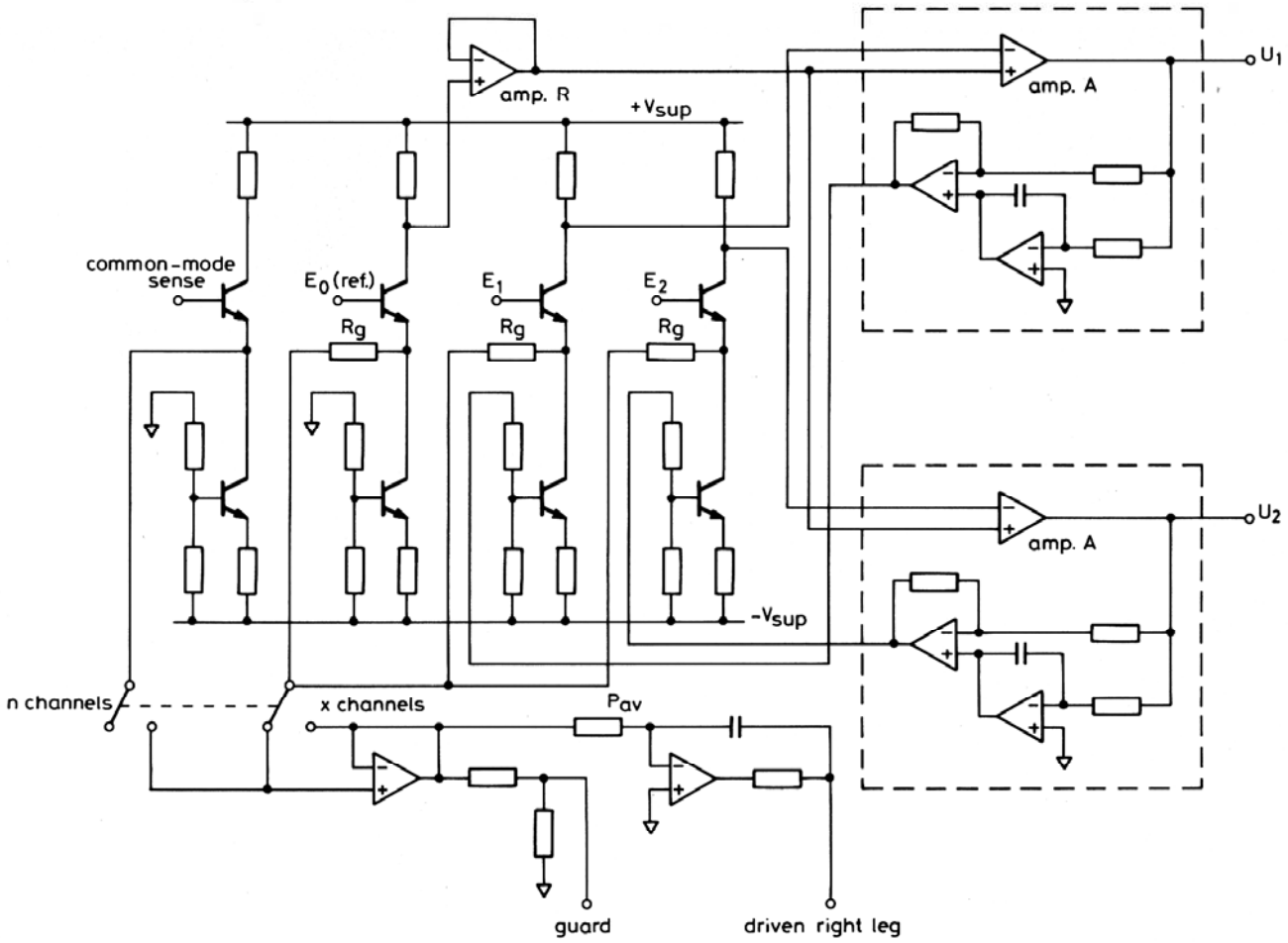

Fig. 3 *Simplified schematic of a multichannel instrumentation amplifier with discrete transistors in the input stage. The circuit is based on the one-channel design of Fig. 2. The amplifier is equipped with guarding and driven right leg circuits and an additional common-mode-sense input stage*

common-mode-sense electrode). The 'average' of the input voltages (= common-mode voltage) is obtained by an extra common-mode-sense electrode and an extra input section. A low-impedance version of the common-mode-sense input signal is used to drive the coupling point P_{av}. When operating in this mode, the voltage of point P_{av} is not controlled by the reference and measuring input signals. Therefore, the reference and measuring sections can all work independently. The number of electrodes used can be chosen freely and malfunctioning of one of the electrodes will not influence the signals derived by the other electrodes. A drawback of this operation mode is that optimum common-mode reduction is achieved only if the common-mode-sense electrode measures the actual average input signal, which will never be the case. In practice this results in a (slight) reduction of the common-mode rejection ratio (CMRR).

7 Discussion

It was experienced that some points needed special attention if the one-channel design (Fig. 2) has to be expanded into a multichannel design (Fig. 3).

In a one-channel instrumentation amplifier the two input transistors can be chosen as a monolithic pair, which ensures good matching (high CMRR) and good tracking of the two transistors with temperature (low drift). The multichannel design (Fig. 3) needs an $n + 1$ matched transistor array (n is the number of channels in a module), which is currently not available in the quality range needed. However, the matching between different LM194 pairs proved good enough to ensure a CMRR of at least 86 dB (approximately 10 dB less than possible with a monolithic matched pair). The use of the thick-film technique helps to reduce temperature differences between the different transistor pairs because the ceramic substrate on which all parts were mounted has very good heat-conducting properties. In addition, all the transistors are situated close together in the thick-film layout (see Fig. 4). Moreover, the offset voltages produced by temperature gradients are cancelled by the DC suppression circuit.

An extra buffer (operational amplifier amp. R in Fig. 3) is included in the reference section to prevent degradation of the CMRR caused by the load presented to the reference section by a large number of interconnected operational amplifier inputs. The extra buffer ensures the equality of common-mode currents in all sections while the noise contribution is insignificant because (differential mode) signals are already amplified more than 20 dB at the point where the buffer is incorporated into the circuit.

8 Results

A thick-film module (60 × 40 × 7 mm) has been developed which contains an eight-channel version of the amplifier described above, together with a multiplexer (Fig. 4). The noise spectrum of one of the prototype modules is given in Fig. 5. It should be noted that the $1/f$ corner frequency is approximately 1 Hz, which is considerably lower than offered by currently available low-noise operational amplifiers (the industry standard OP27 (PMI) low-noise operational amplifier has a $1/f$ corner frequency of 2·7 Hz). Because of the exceptionally low $1/f$ noise of the input transistors (LM194, corner frequency < 0·1 Hz), the $1/f$ corner frequency of the modules is determined by the excess noise of the resistors (see Appendix 2). The use of

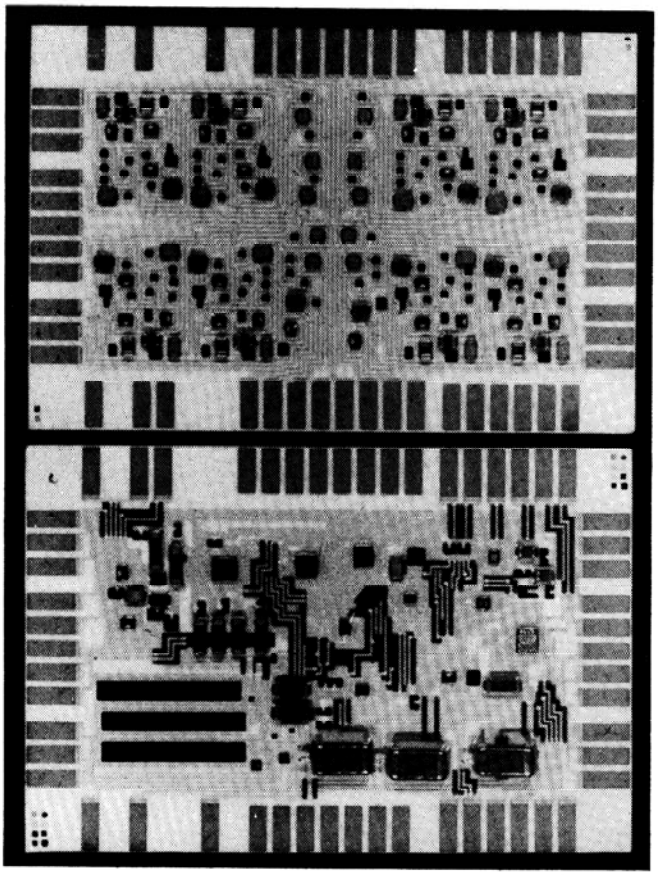

Fig. 4 *Photograph of the eight-channel amplifier (above) and multiplexer (below). The 10-input transistor pairs are placed in the central region of the amplifier layout. The thick-film substrates are assembled back to back to form a compact module*

very high quality thin-film chip resistors (Reinhardt Microtech AG, model URA) proved to be essential in achieving low noise.

Two or four modules can be coupled to make a 16- or 32-channel system with one multiplexed output. More modules can be coupled, but the internal multiplexer can only handle up to 32 channels. Common-mode-sense and reference inputs can be used in different configurations to obtain alternative reference choices. For example: with two modules, a 16-channel ECG front end with standard Wilson Central Terminal (WCT) reference (WILSON *et al.*, 1934) can be formed. Guarding and driven right leg circuits (METTING VAN RIJN *et al.*, 1990) in each module ensure that the mains interference is lower than the noise level of the amplifier in almost any situation. A module (eight channels with a multiplexer, 40 mW) operates for 48 h on two standard 9 V radio batteries (110 mA h each).

Acknowledgment—This work was supported by the Dutch Technology Foundation (STW).

References

ALMASI, J. J. and SCHMITT, O. H. (1970) Systemic and random variations of ECG electrode impedance. *Ann. NY Acad. Sci.*, **170,** 509–519.

CLARK, J. W. (1978) The origin of biopotentials. In *Medical instrumentation: application and design.* WEBSTER, J. G. (Ed.), Houghton Mifflin Co., Boston, 184–207.

COOPER, R., OSSELTON, J. W. and SHAW, J. C. (1969) *EEG technology.* Butterworth, London, 14–22.

DUFF, T. A. (1980) Topography of scalp recorded potentials by stimulation of the digits. *Electroenceph. Clin. Neurophysiol.*, **49,** 452–460.

DUFFY, F. H. (1982) Topographic display of evoked potentials: clinical applications of brain electrical activity mapping (BEAM). Evoked potentials. *Ann. NY Acad. Sci.*, **388,** 183–196.

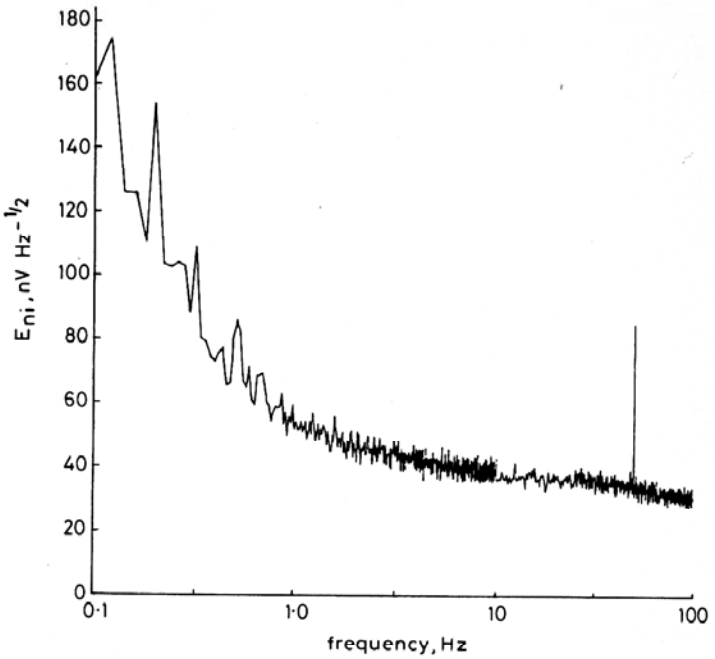

Fig. 5 *Noise spectrum of a thick-film module (source resistors 1 kΩ). The area under the curve amounts to 0·35 μV RMS and represents the equivalent input noise voltage in a bandwidth of 0·1–100 Hz (Data Precision 2000 wave analyser; different sample rates were used above and below 10 Hz)*

GEDDES, L. A. (1972) *Electrodes and the measurements of bioelectric events.* John Wiley & Sons, New York, 44–94.

GEDDES, L. A. and BAKER, L. E. (1989) *Principles of applied biomedical instrumentation,* 3rd edn. John Wiley & Sons, New York, 677–743.

GRAEME, J. G. (1977) *Designing with operational amplifiers: application alternatives.* McGraw-Hill, New York, 31–35.

GRIMNES, S. (1983) Impedance measurement of individual skin surface electrodes. *Med. & Biol. Eng. & Comput.*, **21,** 750–755.

GRUZELIER, J. D., LIDDIARD, D., DAVIS, L. and WILSON, L. (1988) Topographic mapping of electrocortical activity in schizophrenia during directed nonfocussed attention recognition memory and motor programming. In *Functional brain imaging.* PFURTSCHELLER, G. and LOPEZ DA SILVA, F. H. (Eds.), Hans Huber Publishers Inc., Lewiston, New York, 181–186.

HAMSTRA, G. H., PEPER, A. and GRIMBERGEN, C. A. (1984) Low-power, low-noise instrumentation amplifier for physiological signals. *Med. & Biol. Eng. & Comput.*, **22,** 272–274.

HUHTA, J. C. and WEBSTER, J. G. (1973) 60-Hz interference in electro-cardiography. *IEEE Trans.*, **BME-20,** 91–101.

METTING VAN RIJN, A. C., PEPER, A. and GRIMBERGEN, C. A. (1990) High-quality recording of bioelectric events. Part 1 Interference reduction, theory and practice. *Med. & Biol. Eng. & Comput.*, **28,** 389–397.

MORRISON, R. (1977) *Grounding and shielding techniques in instrumentation.* John Wiley & Sons, New York, 132–133.

MOTCHENBACHER, C. D. and FITCHEN, F. C. (1972) *Low-noise electronic design.* John Wiley & Sons, New York, 37–38, **182,** 206–216.

NELSON, C. T. (1980) Supermatched bipolar transistors improve DC and AC designs. *EDN*, 5th Jan., 115–120.

O'BRIEN, M. J., VAN EYKERN, L. A. and PRECHTL, H. F. R. (1983) Monitoring respiratory activity in infants, a non intrusive diaphragm EMG technique. In *Non-invasive measurements: 2.* ROLFE, P. (Ed.), Academic Press, London, 131–177.

PACELA, A. F. (1967) Collecting the body's signals. *Electronics*, **40,** (14), 103–112.

REEK, E. J., GRIMBERGEN, C. A. and VAN OOSTEROM, A. (1984) A low-cost 64 channel microcomputer based data acquisition system for bedside registration of body surface maps. Proc. 11th Int. Congr. Electrocardiol., Caen, France, 17th–20th July, 37–38.

ROSELL, J., COLOMINAS, J., RIU, P., PALLAS-ARENY, R. and WEBSTER, J. G. (1988) Skin impedance from 1 Hz to 1 MHz. *IEEE Trans.*, **BME-35,** 649–651.

SERGENT, J. E. (1981) Understanding the basics of thick-film technology. *EDN*, 14th Oct., 341–349.

SILVERMAN, D., MASLAND, R. L., SAUNDERS, M. G. and SCHWAB, R. S. (1969) Minimal electroencephalographic recording techniques in suspected cerebral death. *Electroenceph. Clin. Neurophysiol.*, **29,** 731–732.

SMIT, H. W., VERTON, K. and GRIMBERGEN, C. A. (1987) A low-cost multichannel preamplifier for physiological signals. *IEEE Trans.*, **BME-34,** 307–310.

SPEKHORST, H. and SIPPENSGROENEWEGEN, A. (1990) Body surface mapping during percutaneous transluminal coronary angioplasty: QRS changes indicating regional conduction delay. *Circ.*, **81,** 840–849.

TOBEY, G. E., GRAEME, J. G. and HUELSMAN, L. P. (1971) *Operational amplifiers: design and applications.* McGraw-Hill, New York, 205–207.

WILSON, N. F., JOHNSTON, F. E., MACLEOD, A. G. and BARKER, P. S. (1934) Electrocardiograms that represent the potential variations of a single electrode. *Am. Heart J.*, **9,** 447–458.

WINTER, B. B. and WEBSTER, J. G. (1983) Driven-right-leg circuit design. *IEEE Trans.*, **BME-30,** 62–66.

WONG, Y. G. and OTT, W. E. (1976) *Functional circuits: design and applications.* McGraw-Hill, New York, 42–45.

Appendix 1

Dimensioning the amplifier circuit

The choice of currents and resistor values (Fig. 2) is determined by a compromise between a number of parameters. For example, choosing the components with respect to the lowest possible equivalent input noise may lead to an amplifier with low DC and common-mode input range and a high input bias current. Therefore special attention was paid to the optimal choice of parameters to achieve a balanced performance.

Selection of R_g and I_e

An input bias current I_{bias} smaller than 50 nA was demanded. Because the transistors used (LM194) have a current gain h_{FE} of approximately 400, the upper limit of the emitter current I_e of the transistors in the input stage is

$$I_e < h_{FE} I_{bias,\,max} = 2 \times 10^{-5}\ \text{A} \tag{1}$$

The amplifier should be capable of handling a differential mode direct input voltage of at least 200 mV. This voltage is also present between the emitters of T_1 and T_2, producing a current through the two resistors R_g‡‡. The maximum magnitude of this current defines the maximum differential-mode direct input voltage. A maximum differential mode direct input voltage with E_1 positive is handled with transistor T_4 not conducting (base of T_4 at $-V_{sup}$). In this case, through both transistors T_1 and T_2 there flows a current $I_e/2$ (I_e is the emitter current through the transistors when there is no direct offset voltage at the inputs), and the current through the two resistors R_g is also $I_e/2$. Consequently, the maximum differential mode direct input voltage is $V_{DC} = (I_e/2)2R_g$. Because a maximum differential-mode DC input range of 200 mV was demanded, the emitter current should fulfil

$$I_e > \frac{V_{DC,\,max}}{R_g} = \frac{0{\cdot}2}{R_g}\ \text{A} \tag{2}$$

The equivalent input noise voltage of the amplifier is dominated by shot-noise currents of the four transistors in the input stage. A more detailed description of the various shot-noise currents and their influence on the equivalent input noise is found in Appendix 2. It is convenient to use one of its results (eqn. 6):

$$E_{ni} = 2\Gamma R_g \sqrt{2qI_e\Delta f}\ \text{V}$$

where $\Gamma = 0{\cdot}5$ (Γ is a correction factor to account for the interaction between the charge carriers, see Appendix 2).

A demanded equivalent input noise voltage E_{ni} of less than 0·35 μV RMS in a bandwidth of 0·1–100 Hz results in a third relationship containing I_e:

$$I_e < \frac{(E_{ni,\,max})^2}{R_g^2\, 8\Gamma^2 q\Delta f} = \frac{4 \times 10^3}{R_g^2}\ \text{A} \tag{3}$$

Finally, a differential-mode input impedance Z_d larger than 10 MΩ was demanded. The differential mode input voltage V_d produces a current I_d through the two resistors R_g($V_d = 2R_g I_d$). The feedback circuit will regulate the current source around T_4 in such a way that in both transistors T_1 and T_2 there flows an extra current I_d. As a result, in both transistors there flows an extra input (base) current $I_{d,\,in}$ of I_d/h_{FE}. With the differential-mode input resistance defined as $Z_d = V_d/I_{d,\,in}$, an upper limit for R_g is found:

$$R_g = \frac{V_d}{2I_d} = \frac{V_d}{2I_{d,\,in}h_{FE}} > \frac{Z_{d,\,min}}{2h_{FE}} = \frac{10^5}{8}\ \Omega \tag{4}$$

Relns. 1–4 are plotted in Fig. 6. The central area represents the permitted combinations of R_g and I_e.

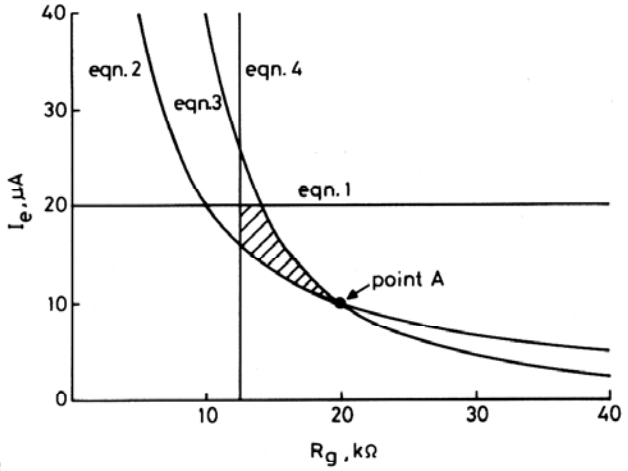

Fig. 6 *Relationship between the emitter current I_e of the input transistors and the gain setting resistor R_g for constant input bias current of 50 nA (eqn. 1), constant DC range of 200 mV (eqn. 2), constant equivalent input noise voltage of 0·35 μV RMS (eqn. 3) and a constant differential-mode input impedance of 10 MΩ (eqn. 4). The amplifier surpasses the demanded specifications if R_g and I_e are chosen inside the hatched area. Point A represents the choice that was made for the modules produced*

It was decided to optimise the design with respect to the lowest possible input bias current and highest possible differential-mode input impedance. Consequently an emitter current I_e of 10 μA and gain resistors R_g of 20 kΩ were chosen (point A in Fig. 6).

Selection of R_e and R_c

The first amplifier stage has a closed-loop gain of R_e/R_g. This gain has to be at least 10 to prevent a substantial influence of noise from the feedback circuit (signal coupled to the base of transistor T_4). Because R_g was already set at 20 kΩ, R_e should be at least 200 kΩ. A larger value will decrease the common-mode input range while extra noise reduction is not achieved. R_e is therefore chosen 200 kΩ.

The open-loop gain of the first amplifier stage is determined by the ratio R_c/R_g. The open-loop gain of the first stage should be higher than 10 otherwise the noise contributions of operational amplifier amp. A will dominate. However, a large value for resistor R_c will limit the common-mode input range. R_c = 400 kΩ (open-loop gain of the first stage is 20) offers a good compromise between low noise and a large common-mode input range.

Appendix 2

Noise

All devices used in the amplifier, the capacitors excepted, introduce noise. Furthermore, each device generates different types of noise. The main contributions of these noise sources to the equivalent input noise voltage are evaluated in the following sections.

‡‡ *The gain resistor R_g is split in two to simplify the extension of the one-channel design in Fig. 2 to the multichannel design in Fig. 3. The derivations in the appendices are based on the one-channel design. However, the results are also valid for the multichannel version*

Excess noise in thick-film resistors

When a current flows through a resistor, extra noise is added to the ever present thermal noise because the current flow is not completely uniform. This so-called excess noise has a $1/f$ spectrum; the noise energy in each frequency decade is constant. The amount of noise depends on the physical properties of the resistive material. The quality of a resistor in this respect is indicated by the noise index NI, which gives the amount of noise in μV RMS per frequency decade with a 1 V direct voltage drop across the resistor.

Thick-film resistors made of resistive ink, which are normally used in thick-film circuits, produce high amounts of excess noise. We measured noise indexes of 3–5. Calculations showed that the demanded noise specifications (0·35 μV RMS, bandwidth 0·1–100 Hz) of the amplifier could only be met if resistors with an NI of less than 0·5 were used. It proved impossible to reach such a low NI with thick-film resistors. Consequently, all critical resistors in the modules are high-quality thin-film chip resistors with an NI lower than 0·1.

Shot-noise in the transistors

The main noise source in a high-quality semiconductor is shot noise. While other transistor noise sources ($1/f$ noise, excess noise, thermal noise) may be reduced with a careful production process, the amount of shot noise is determined only by the magnitude of the chosen currents in the transistor. Shot noise is caused by the discrete character of the charge carriers. The available number of charge carriers in a certain time interval is subjected to statistical variations. The magnitude of these variations, and therefore the shot-noise current that is generated, can be predicted on statistical grounds:

$$i_{sh} = \Gamma\sqrt{2qI\Delta f}\ \text{A} \tag{5}$$

The factor Γ is equal to unity when the charge carriers move totally independently of each other. However, in most electronic devices this is not the case. The space charge of the charge carriers will counteract variations in current flow; hence the measured noise is lower than expected. From our noise measurements we derived a Γ of 0·5 for the transistors used (LM194) (In the literature transistor Γ values are hardly referenced.)

Both the collector and base currents have shot-noise components. The base currents, however, do not add significantly to the equivalent input noise voltage because the input bias currents are small (25 nA, see Appendix 1) and the source impedances (the electrodes for T_1 and T_2; $R_1 \| R_2$ for T_3 and T_4) are not very high.

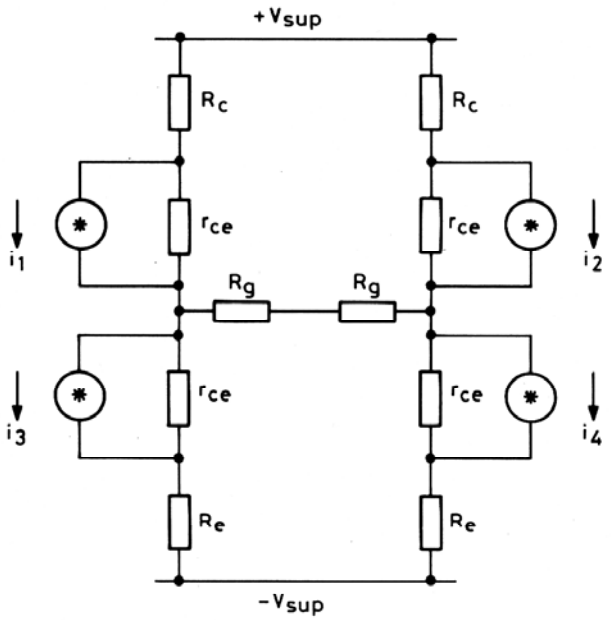

Fig. 7 *Simplified equivalent diagram of the input stage of the amplifier in Fig. 3. The transistors are represented by shot-noise current sources i_1–i_4 and noiseless resistors r_{ce}. Approximately half of each noise current is flowing through resistors R_g ($r_{ce} \gg R_e, R_c, R_g$)*

The collector to emitter current in an n-p-n transistor is controlled by the number of electrons that are injected in the base region and collected by the collector. Fluctuations in the number of electrons that reach the collector in a certain time interval cause a shot-noise current according to reln. 1, in which I is the emitter current I_e of the transistor (the small difference between emitter and collector current is neglected). It is now possible to evaluate the noise contributions of the four transistors in the input stage. Each transistor can be represented by a noise current source parallel to a noiseless resistor (the dynamical collector-emitter resistance, approximately 10 MΩ in this case). The four noise sources and all relevant resistances are shown in Fig. 7.

The equivalent input noise voltage that is produced by these noise currents is determined by considering the voltage that each current causes across the resistors R_g. A voltage across the two resistors R_g in series is readily compared with an input voltage. Inspection of Fig. 7 shows that approximately half of the shot-noise current produced by each transistor flows through the resistors R_g. These four noise sources are uncorrelated, so the mean squares of the noise voltages across the two resistors R_g in series should be added. Finally, an estimation of the equivalent input noise voltage of the amplifier caused by the four shot-noise currents is found:

$$E_{ni} = \sqrt{4(i_{sh}/2)2R_g} = 2\Gamma R_g\sqrt{(2qI_e\Delta f)}\ \text{V}$$
$$= 0{\cdot}35\,\mu\text{V RMS, bandwidth } 0{\cdot}1\text{–}100\,\text{Hz} \tag{6}$$

where

$$\Gamma = 0{\cdot}5,\ I_e = 10\,\mu\text{A},\ R_g = 20\,\text{k}\Omega$$

It can be calculated that, with an emitter current of 10–30 μA and an R_g of 10–30 kΩ (see Appendix 1), all other noise sources in the design (excess and thermal noise of the resistors, noise of the operational amplifiers) are negligible with respect to the shot noise of the four transistors in the input stage (equivalent input noise voltage = 0·2–0·9 μV RMS, bandwidth 0·1–100 Hz).

Authors' biographies

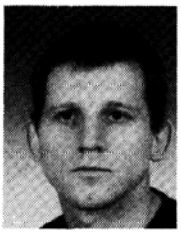

A. C. Metting van Rijn was born in 1959. In 1987 he received his degree in Physics from the University of Amsterdam. Currently he is with the Laboratory of Medical Physics & Informatics of the University of Amsterdam. His research interests centre on medical electronics and transducers. Since 1989 he has been working on a project for the development of miniature biomedical instrumentation, on a grant from the Technology Foundation (STW).

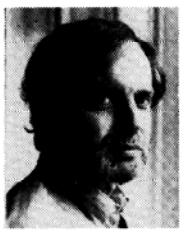

Abraham Peper (51) is a physicist at the Laboratory of Medical Physics of the University of Amsterdam. He received a Ph.D. degree for his work on the recording of His-Purkinje potentials at the body surface. At present he is engaged in various projects in the field of cardiology, instrumentation for cardiological and ultrasound research and the modelling of biological processes, on which subjects he has published several papers.

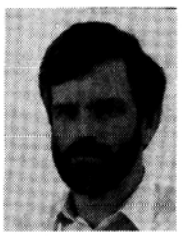

Cornelis A. Grimbergen (43) is a physicist at the Laboratory of Medical Physics of the University of Amsterdam. After receiving his Ir. degree in Electrical Engineering at the Delft University of Technology he was active in research in solid-state physics, resulting in a Ph.D. degree in 1977 from the University of Groningen. From 1977 he has been with the Medical Physics Laboratory, working in the fields of medical instrumentation, biomedical signal processing and biological system modelling.